16th ICAAR LISBOA 2020-2022

16th International Conference on
Alkali-Aggregate Reaction in Concrete
Lisboa | LNEC | Portugal | 31 May - 2 June 2022

http://icaar2020-2022.lnec.pt

# Development of hybrid HSCT-FE models to study the behavior of large dams due to concrete swelling

**Miguel Rodrigues [(1)], Sérgio Oliveira [(2)], Jorge Proença [(3)]**

*(1) Laboratório Nacional de Engenharia Civil, Lisbon, Portugal, mrodrigues@lnec.pt*

*(2) Laboratório Nacional de Engenharia Civil, Lisbon, Portugal, soliveira@lnec.pt*

*(3) CERIS – Instituto Superior Técnico, Lisbon, Portugal, jorge.m.proenca@tecnico.ulisboa.pt*

## Abstract

*The safety control of large dams is based on the behavior monitoring over time and on the comparison between predicted and observed behavior. The most commonly used models for dam behavior prediction are FE models and for the interpretation of observed data are the effects separation models of the type Hydrostatic-Seasonal-Time (HST) models. These models allow to separate the effects of the main loads, which are: the hydrostatic pressure elastic effect (H), seasonal effects due to temperature variations (S) and the time effects (T). Although the HST models offer an important contribution for the understanding of dams behavior and for the calibration of numerical models like the Finite Elements Models (FEM), they are not able to identify pathological behavior like the one produced by the swelling reactions. Operating dams, considering the concrete types used and their usual environmental operation conditions, in terms of temperature and humidity, are structures prone to swelling development over time, which, in the worst situations, can lead to the decommissioning of a dam.*

*In this paper is presented a hybrid model of the type HSCT-FE, developed in LNEC-DBB. This hybrid model allows the separation of the main effects, namely: the hydrostatic pressure elastic effect (H), seasonal effects due to environmental temperature variations (S), creep effect due to the hydrostatic pressure (C), and other time effects (T), like creep due to the self-weight and the swelling effect.*

*Cabril dam, a double curvature arch dam (132 m high) is presented as the case study. This dam presents structural cracking and signs of swelling. Gel exudations at the upper observation galleries can be observed. The proposed hybrid HSCT-FE models are able to separate the swelling reactions effect presenting a quantitative evolution coherent with the observed swelling values obtained from the isolated strain gauges in dam body.*

***Keywords**: swelling effects; creep effects; seasonal effects; HSCT-FE models; large concrete dams*

## 1. INTRODUCTION

The safety control of operating dams is based on the comparison between observed data from monitoring systems and numerical data from mathematical models developed to simulate/predict the dam behaviour over time. Semi-statistical models for effects separation are usually adopted for the direct analysis of observed data, Hydrostatic-Seasonal-Time (HST) or Hydrostatic-Seasonal-Creep-other Time effects (HSCT) models. The Finite Elements Models (FEM), based on the fundamental equations of structural mechanics are generally used for dam behaviour simulation and prediction.

For the detection of abnormal behaviour derived from the pathological effects, *e.g*. concrete swelling effects, it is necessary to use robust separation of effects models capable of distinguishing normal time effects, related to viscoelasticity, from other time effects, *e.g*., related to concrete swelling.

In this paper, a hybrid HSCT-FE model is proposed, and it is applied to the case study of Cabril dam.

## 2. MODELS FOR EFFECTS SEPARATION OF THE TYPE HST, HSCT AND HSCT-FEM

### 2.1 Classic effect separation models: HST type models

The history of displacement *d*, at a given point in a dam, can be obtained with an effect separation model of the HST type, adjusting a given function to the observed values by linear regression, using the Least Squares Method (LSM), in this case a function of three variables associated with the main actions: one

representative of the variations in the reservoir level, *h*; another representative of seasonal thermal variations, which may be the day of the year or the average daily temperature (air temperature or concrete temperature, at a given point or in a given area of the dam body), *S*; and one last variable, representing the total time elapsed since construction, *t*. Thus, the regression equation of an HST model can be generically written as follows

$$d = d_H(h) + d_S(s) + d_T(t) + k \quad (1)$$

where:

$d_H(h)$ – is the displacements component related to the reservoir water level variation (hydrostatic pressure effect); variable *h* usually stands for the water height counted from the empty reservoir elevation, nevertheless, it can also represent a water height counted from another reference, generally higher than the empty reservoir water level; additionally, *h* might represent the mean weekly or monthly water height previous to the considered observation date (usually admissible for the water flow and pressure study at the foundation).

$d_S(s)$ – is the displacements component related to the seasonal thermal variations; as referred, variable *s* can represent a certain time of the year, $s = \overline{t}$, where $\overline{t}$ is counted in days from January first $\left(0 < \overline{t} < 365,25\right)$, *s* can also represent the average daily air temperature $s=T_{air}$ (with or without delay to simulate the heat flux inside the concrete) or the concrete temperature measured in a given thermometer, $s=T_{conc}$.

$d_T(t)$ – is the time effects component, which may include: (i) the hydrostatic pressure creep effect; (ii) the self-weight creep effect; (iii) the swelling reactions effect; (iv) the foundation movements effect; and (v) differed effects related with the structural properties variation occurred over time; variable t is usually counted in days from the reference date admitted as time absolute origin (commonly coinciding with a date at the end of the construction period, Figure 2.1); and

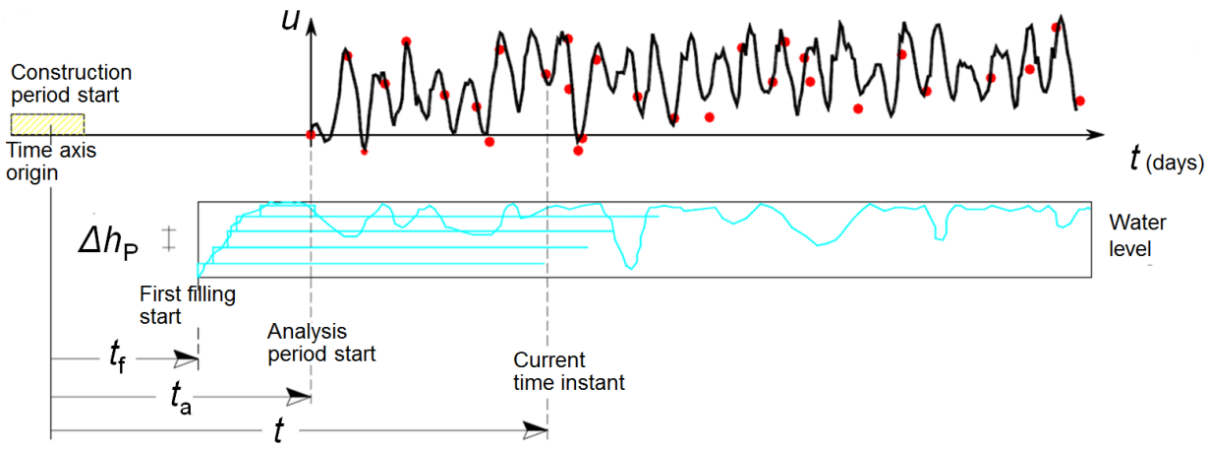


Figure 2.1: Time variable in a displacement analysis. Definition of the time axis origin, first filling, analysis period start and current time instant

*k* – is a constant that is introduced due to the fact that the observed values correspond to values for a given initial epoch taken as reference; constant *k* can be given by an expression dependent on the observed value $d_{obs,e_a}$, at epoch $e_a$ correspondent to the beginning of the analysis period, which can be written as:

$$k = d_{obs,e_a} - \left[ d_H\left(h_{e_a}\right) + d_S\left(s_{e_a}\right) + d_T(t_{e_a}) + r_{e_a} \right] \quad (2)$$

For each observation epoch *e*, characterized by $h=h_e$, $T=T_e$ and $t=t_a$, the observed displacement component, $d_{obs}=d_{obs}(h_e,s_e,t_e)$, will coincide with the displacement calculated by the model at the same epoch, $d_{obs}=d_{obs}(h_e,s_e,t_e)$, subtracted the residual $r_e$ from the statistical adjustment of Equation 1 to the observed values at the various epochs.

## 2.2 Consideration of creep: HSCT type models

The HSCT models distinguish themselves from the HST models by allowing to explicitly consider the viscoelastic response associated with the hydrostatic pressure (Creep) [1], therefore, making their name progress to: Hydrostatic, Seasonal, Creep and other Time effects models (HSCT).

One of the main disadvantages of the classic HST effects separation models is that they do not allow the time effects to be separated into several terms. The long-term analysis of the observed behaviour in most concrete dams shows that the effects of time corresponds to the overlap of several parcels, namely: a portion of creep associated with hydrostatic pressure, a portion of creep associated with the self-weight, or even, in cases of dams with swelling problems, a portion associated with the progressive effect of swelling. To exemplify the interest of the HSCT models, we can refer to the case of the radial displacements observed in arch dams, in which the creep component associated with the hydrostatic pressure and swelling can cause progressive displacements in opposite directions (*e.g*. creep causes displacements downstream and swelling upstream), which can result in these two terms masking each other out, “hiding” the swelling pathological behaviour in the process. The HSCT models are able to detect the whole pathological component. Due to the fact that most dams suffer, at a certain degree, from swelling problems, it is essential that the models used to analyse the observation data allow the quantification of the different components involved in the so-called effects of time.

As mentioned above, the time effect that can be conveniently separated from the other time effects is precisely the creep effect associated with the hydrostatic pressure. This effect has a known dependence on the water level evolution, in addition to the well-known dependence on the time variable. Thus, in most cases where the creep function is known in an approximate way, it is possible to formulate a new type of effect separation models that incorporates knowledge from the physical correlation between the elastic and deferred terms associated with variations of the reservoir water level.

Due to the concrete viscoelastic behaviour, for applied forces such as the hydrostatic pressure or the self-weight, the displacement field increases over time by creep influence (for imposed deformations, the viscoelastic behaviour is associated with the relaxation of tensions).

### 2.2.1 Hydrostatic pressure elastic effect

The hydrostatic pressure elastic effect is usually described by polynomial expressions, such as

$$d_H(h) = a_1 h^4$$
$$d_H(h) = a_1 h^4 + a_2 h^3 \quad (3)$$
...

or involving exponential functions, like the following

$$d_H(h) = a_1\left(e^{h/c_f} - 1\right)$$
$$d_H(h) = a_1\left(e^{h/15} - 1\right) + a_2\left(e^{h/20} - 1\right) \quad (4)$$
...

where:

$h$ - is the water height in the reservoir above a reference level conveniently chosen, for example the foundation central blocks level or the empty reservoir level;

$a_i$ – are the regression coefficients to be estimated; and

$c_f$ - is a shape coefficient related to the exponential curve curvature, generally assuming values between 10 and 30.

Therefore, the hydrostatic pressure elastic effect can be described by polynomial or exponential expressions, both dependent of the water height, $h$, above the value adopted as reference value, and normally with zero (or almost zero) derivative at the origin ($h$=0).

When using polynomial functions, experience told that the use of monomials, or binomials of the fourth degree, led to good results in the analysis of dam displacement histories. However, it has been found that in certain cases, better adjustments can be obtained using exponential functions (Eq.4), especially in the displacement analysis of arch dam points located away from the central section, where, for low reservoir levels, the effect of hydrostatic pressure would have been negligible, as shown in Figure 2.2.

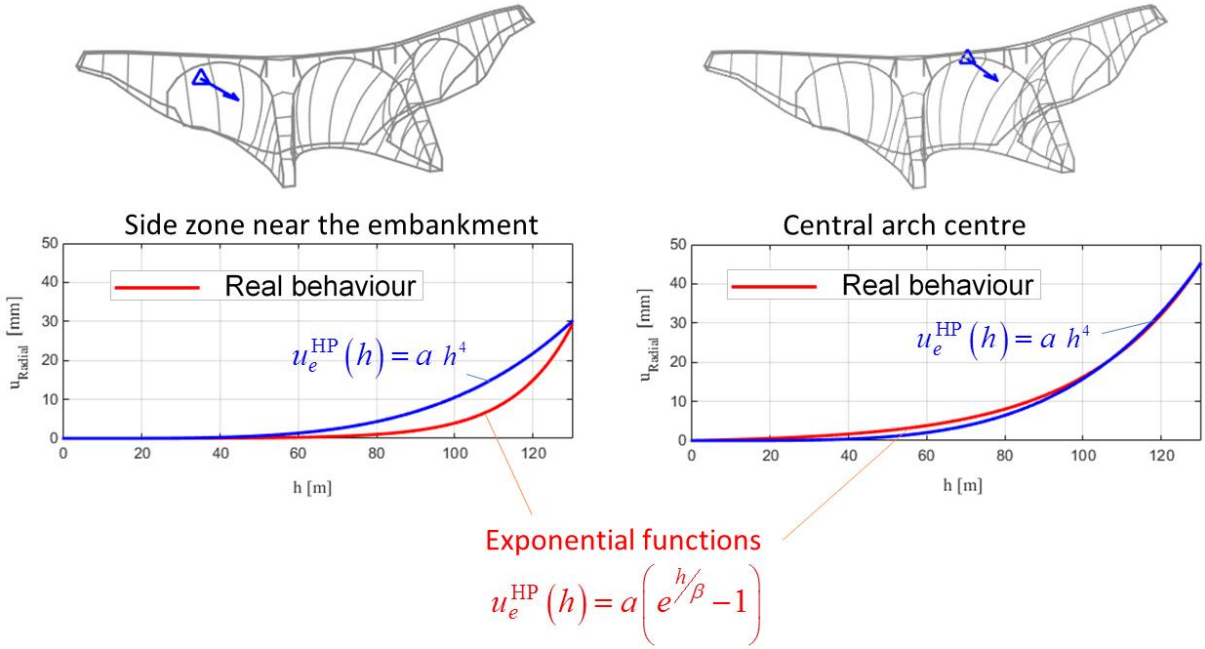


Figure 2.2: Exponential function usage advantage to describe the observed behaviour in arch dams near the embankments. The exponential function adjustment is coincident with the structure real behaviour not only at the top of central section but also near the embankment, whereas, the polynomial function has difficulty to adjust itself to the real behaviour near the embankment

### 2.2.2 Temperature effect

For the influence of air temperature changes in the structural response of dams, the seasonal effect (due an annual thermal wave or, in tropical climates, to a composite wave resulting from the combination of an annual wave and an half-yearly wave) is, in general, dominant, and, in certain cases, it may be convenient to also consider the effect of thermal waves of shorter periods, such as the daily thermal wave for the study of small arch dams. For the structural response effect estimation to the seasonal temperature variations using separation of effects models (which correspond to annual thermal waves, which are obviously not perfect harmonics, and which, in general, can have an average value and amplitude significantly different from year to year), it is generally admitted that, in terms of displacements, the response is proportional to the variations in the measured air temperature (Equation 5). In general, the average daily air temperature is considered with a delay (*e.g.* 30 days, see Figure 2.3), alternatively it can be considered the average daily temperature measured on the dam body, at a point located, *e.g.*, at the dam upper zone, at a distance from the downstream face of about 1/3 of the thickness. Sometimes, in simpler separation of effects models, the seasonal effect due to temperature variation can be estimated through perfect harmonic waves with an annual period (or annual and half-yearly periods, for the case of dams located in tropical climates). In cases where this simplifying hypothesis is adopted, harmonic functions of an annual period (or annual and half-yearly) are used, depending only on the day of the year, counted from January 1 [2], as indicated by Equation 6 and Equation 7.

$$d_S(s) = b.s\,, \qquad s = T_{\text{air},lag} \quad \text{or} \quad s = T_{P,\text{concrete}} \tag{5}$$

$$d_S(s) = b_1 \cos\left(\frac{2\pi s}{365.25}\right) + b_2\, \text{sen}\left(\frac{2\pi s}{365.25}\right) \tag{6}$$

$$d_S(s) = b_1 \cos\left(\frac{2\pi s}{365.25}\right) + b_2 \text{sen}\left(\frac{2\pi s}{365.25}\right) + b_3 \cos\left(\frac{2\pi s}{182.625}\right) + b_4\, \text{sen}\left(\frac{2\pi s}{182.625}\right) \tag{7}$$

where: $0 < s = \overline{t} < 365.25$ days

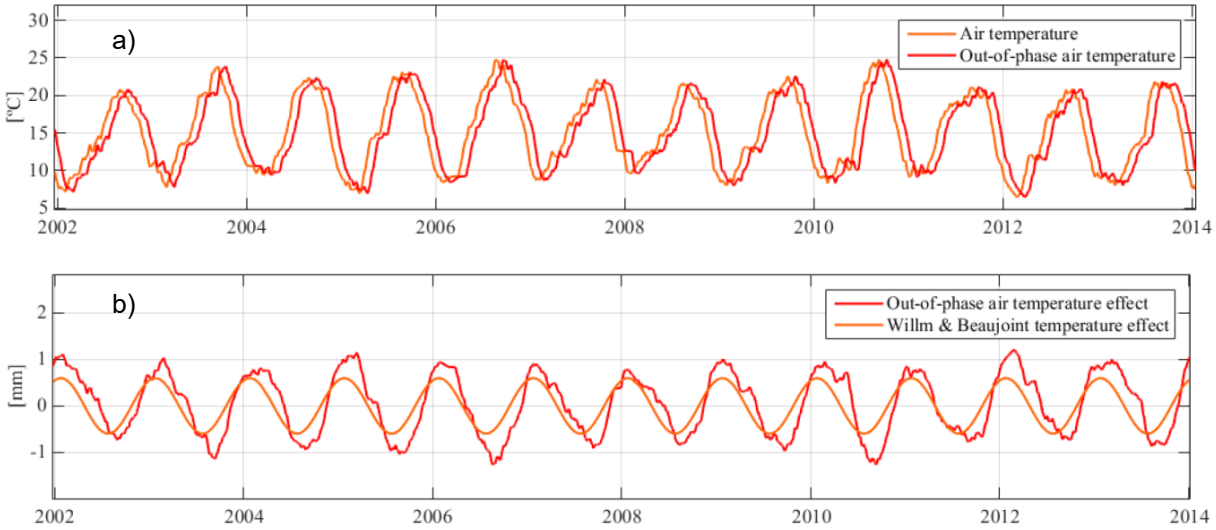


Figure 2.3: Thermal effect estimation. a) Observed air temperature and delayed observed air temperature. b) Thermal effect estimations by the delayed observed air temperatures and by the use of Willm and Beaujoint hypothesis

When $s=T_{air,lag}$ is considered it corresponds to adopting, for variable $s$, the delayed daily average air temperature with a delay *lag*, $T_{air,lag}=T_{air}(t\text{-}lag)$, as is shown in Figure 2.3a. It is usual to adopt about 20 to 30 days of lag (delay), e.g. *lag*=25 days. When $s=T_{P,concrete}$ is considered it corresponds, as mentioned above, to the adoption of the average daily temperature measured at a dam point.

### 2.2.3 Hydrostatic pressure differed effect

As mentioned, an important limitation of the HST type models is their incapacity to separate the time effect into multiple components. In fact, generally, the time effect encompasses several important components that are worth knowing separately. In particular, it is interesting to identify possible pathological components, as it is the case of the swelling reactions. This component can be well identified by adopting HSCT type models which allows the isolation of the creep component associated with the hydrostatic pressure and also, if necessary, the creep component associated with the self-weight.

If the water level evolution is gradual and eventually with variations, both upwards and downwards, it will be necessary to add, to the elastic component of the hydrostatic pressure effect, in addition to the effect of the thermal field change, a deferred component, time dependent, still associated with the water level variation, due to the viscoelastic behaviour of the material.

Admitting the maturation effect on instantaneous deformations as negligible, as it will occur in many periods of the analysis, and admitting that creep has a linear character in the domain of service loads, with its parameters depending on the load application age, a function can be determined (Equation 8) representing the quotient between the deformation from the deferred term, at age $t$, due to a load applied at age $t'$, and the instantaneous elastic deformation component.

$$\phi(t,t') = J(t,t')E(t) - 1 \tag{8}$$

If it is admitted as an origin date for the concrete age representative of the structure, for the purpose of characterizing its rheological properties, an intermediate date of the dam construction period; consider it a quantity whose observations subject to analysis begin at a time when the concrete age, according to this criterion, is $t_a$.

If the water level evolution over time is represented as a succession of $p$ levels, of amplitude $\Delta h_j=h_j-h_{j-1}$ (Figure 2.4a), applied to age $t_j'$, that is:

$$h(t) = \sum_{j=1}^{p} \Delta h_j \tag{9}$$

the superposition of effects principle validity allows Equation 10 to be obtained considering a polynomial configuration, *e.g.* $d_H(h)=ah^4$, to represent the hydrostatic pressure elastic effect; or Equation 11 to be obtained for an exponential configuration, *e.g.* $d_H(h)=a(e^{h/20}-1)$, to represent the same effect.

$$d_C(h,t) = a\left[ h^4 + \sum_{j=1}^{p} \phi(t,t_j^{'})\,\Delta h_j^4 - \sum_{j=1}^{p'} \phi(t_a,t_j^{'})\,\Delta h_j^4 \right] \tag{10}$$

Where $p$' is the number of levels considered for the water level variation since the beginning of the first filling until epoch $t_a$, correspondent to the beginning of the analysis period ($\Delta h_j^4=h_j^4-h_{j-1}^4$).

$$d_C(h,t) = a\left[ \sum_{j=1}^{p} \phi\left(t,t_j^{'}\right)\left( e^{h_j/20} - e^{h_{j-1}/20} \right) - \sum_{j=1}^{p'} \phi\left(t_a,t_j^{'}\right)\left( e^{h_j/20} - e^{h_{j-1}/20} \right) \right] \tag{11}$$

The graphical representation of the calculation process associated with the hydrostatic pressure creep effect estimation, whose Equation 10 and 11 provide for the discretization at constant load levels, is shown in Figure 2.4a.

### 2.2.4 Other time effects

For the displacement analysis, in what regards the time effects, there are other effects to take into account besides the hydrostatic pressure effect. It might be important to consider the self-weight creep effect and, of course, possible effects associated with pathologies, such as, the development of swelling reactions over time.

Generically, the other time effects displacements can be estimated by Equation 12. This type of time dependent polynomial function (contingent on the number of days after the beginning of the analysis period $t_a$ until the observation date $t$) allows the time effects definition resulting from a combination of different differed phenomenon sources.

$$\begin{aligned} &d_T(h) = c_1\left(t-t_a\right) \\ &d_T(h) = c_1\left(t-t_a\right) + c_2\left(t-t_a\right)^2 \\ &\ldots \end{aligned} \tag{12}$$

The self-weight elastic response cannot be measured on site. This component, unlike other loads, installs itself progressively during construction. This effect might be important to estimate in order to isolate the swelling or foundation movement effects. It is relevant to point out that a recent dam might not present foundation movements and swelling reactions effects, making the other time effects component equal to the self-weight creep effect. In the opposing cases, subtracting the self-weight effect to the observed displacements might make the other preponderant time effect known (swelling or foundation movements). Therefore, it becomes important, before the beginning of a thorough analysis, to know about the existence of swelling behaviour or foundation movements, from what is observed on the isolated strain gauges or on the inverted pendulums and on the borehole extensometers, respectively.

Consequently, as an alternative, when the swelling reactions and foundation movements effects are negligible and characterizing the other time effects component by its usual essentially viscoelastic time phenomenon that are processed monotonically at a successively decreasing rate, Equation 13 logarithmic expression can be used to represent a prevailing self-weight effect.

$$d_T(t) = c_2 \log\left(1+\frac{t}{t_a}\right) \tag{13}$$

Self-weight is a constant gravity force applied to the structure, which provokes a differed response on the dam. Figure 2.4b presents the self-weight effect typical development over time. In the figure, the effect is composed by two components, where the grey area represents the creep displacement component and below, the white area, is represented the elastic response component.

a)

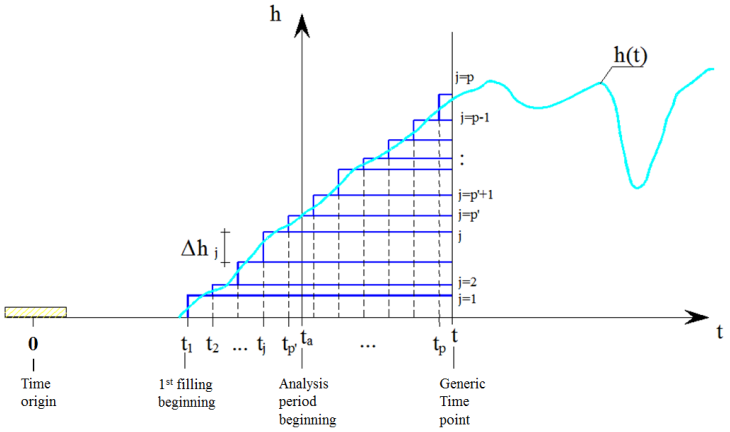


b)

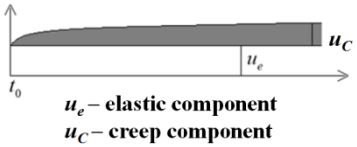


$u_e$ – elastic component
$u_C$ – creep component

$$u^{SW}(t) = u^{SW}_{eFEM} + u^{SW}_{C} = \\ = u^{SW}_{eFEM} + \phi(t,t_0)\,u^{SW}_{eFEM}$$

Figure 2.4: Creep behaviour over time. a) Reservoir level discretizations in intervals (the reference epoch for time counting is approximately coincident with the mean construction period date). b) SW elastic creep component

For the abovementioned case of an identified *a priori* predominant time effect like the swelling reactions or the foundation movements, it might be important to separate those pathological nature effects. To execute that separation using HSCT models, the self-weight creep effect has to be estimated. The referred estimation can be made by the FEM, based on the creep coefficient estimated for the creep law considering the mean creep age for the structure concrete. Hence, with a known time effect component related to the self-weight, it is possible to subtract it to the other effects of time and, that way, it is isolated and, at the same time, identified the desired pathological effect (swelling or foundation movements). Equation 14 presents that calculus possibility.

$$d^{SW}(t) = d^{SW}_{e,FEM} + d^{SW}_{C} = d^{SW}_{e,FEM} + \phi(t,t_0)\,d^{SW}_{e,FEM} \tag{14}$$

As mentioned before, there are many time effects, Equation 15 aims for the swelling reactions effect estimation.

$$d^{exp}(t) = c_3\left(e^{-\frac{t_a^n}{\lambda}} - e^{-\frac{t^n}{\lambda}}\right) \tag{15}$$

The exponential function parameters estimation is executed in order for the swelling action to reach half its total effect, at the end of $t_{hs}$ days, considering $n$=3.258 and $\lambda = t_{hs}^n(n/(n\text{-}1))$. These $n$ values are determined when the swelling effect inflexion point, $t=t_{inf}$ (Figure 2.5) coincides with the point where the swelling reaches half its total effect ($t=t_{inf}=t_{hs}$). At this point, the second derivative in order to variable $t$ of the exponential term is almost zero, which, considering an analysis period coinciding with the origin of the time axis $t_a$=0, it is possible to write:

$$\left(1 - e^{-\frac{t^n}{\lambda}}\right) = 0 \Leftrightarrow \lambda = t_{hs}^n \frac{n}{n-1} \tag{16}$$

Hence, starting from the condition that renders the hypothesis in which half of the total swelling effect occurs at the inflexion point, the abovementioned n value is obtained:

$$f\left(t = t_{inf} = t_{hs}\right) = 0{,}5 \Leftrightarrow 1 - e^{-\frac{n-1}{n}} = 0{,}5 \Leftrightarrow n = 3{,}258 \tag{17}$$

Therefore, the expression related to the displacements due to the swelling reactions are [3]:

$$d^{swe}(t) = c_3\left(1 - e^{-t^n/\beta}\right) \tag{18}$$

$$\beta = t_{hs}^{n} \times n/(n-1), \quad n = 3.258 \quad \text{e} \quad t_{hs}^{n} \simeq 8000 \text{ dias} \tag{19}$$

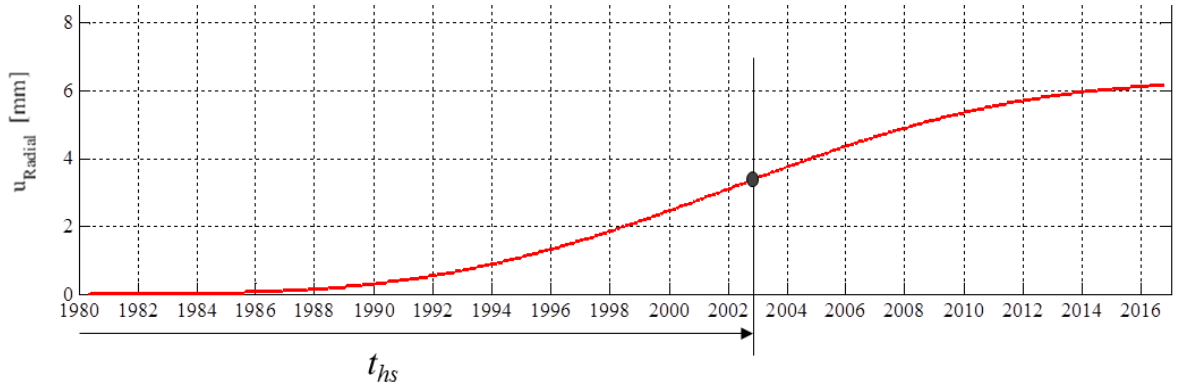


Figure 2.5: Swelling reaction effect representation through a sigmoid type function [3]. The inflexion point represented by $t_{hs}$ is known as half-swelling point or time

This function development over time is presented in Figure 2.5. The sigmoid type curve gives the displacements provoked by the swelling effect, accordingly, it raises slowly over time until the half swelling age, at that moment, the curve changes curvature and, over time, the displacements tend towards stabilization. In this study it was considered a half-swelling age of 15,000 days (approximately 41 years). This value was obtained by a cross analysis between the isolated strain gauges data and the parametric studies performed for the calibration of the regression model. Larive's sigmoid type function is used in this statistical model, to simulate the time evolution of the displacement field of the whole structure (displacement evolution in every point under monitoring). Larive's specific parameters that govern the kinetics of the swelling reactions can be initially inferred from the expected average sigmoide type structural response of the dam, observed and computed by FEM using an initial estimate for swelling values, and then the Larive's parameters can be used as input in a program for expansion prediction until the computed structural response matches the observed behavior for the predicted swelling values.

With the hydrostatic pressure creep effect, self-weight creep effect, swelling reactions effect, all characterized, the remaining important time effects result from foundation movements.

Certain dams display some foundation movements. Equation 20 can be used in order to estimate the foundation movement displacements, where $c_3$ is the regression coefficient. This time effect, only time dependent (just like the swelling reactions effect is), provokes irreversible changes in the structure.

Figure 2.6 shows how the foundation movements provoke smooth and gradual displacements, with a tendency to stabilize over time. Hence, this effect is approximated by a logarithmic type function presented below.

$$d^{\text{FM}}(t) = c_4 \times \log\left(1 + \frac{t}{1000}\right) \tag{20}$$

Figure 2.6 example explains the development over time of component $d^{\text{FM}}$.

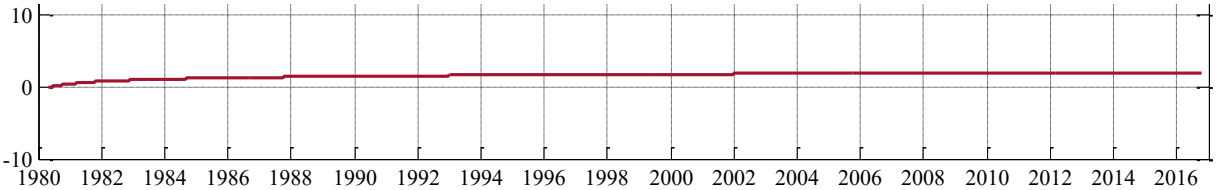


Figure 2.6: Typical foundation movements effect development over time

### 2.2.5 Regression model

Considering what has been mentioned above, the resulting regression equation, for a HSCT type effect separation, would have the following form:

$$d = d_{\mathrm{H}}(h) + d_{\mathrm{S}}(\bar{t}, T) + d_{\mathrm{C}}(h,t) + d_{\mathrm{T}}(t) + k \tag{21}$$

where:

$$d_{\mathrm{T}}(t) = d^{\mathrm{SW}}(t) + d^{\mathrm{swe}}(t) + d^{\mathrm{FM}}(t) + d_{\mathrm{T}}(t) \tag{22}$$

It is important to note that the other time effects component ($d_T(t)$) subdivision requires previous knowledge about the existence of important time effects (*e.g.* swelling reactions effects and/or foundation movements effects).

## 3. ANALYSIS OF CABRIL DAM BEHAVIOR USING HYBRID HSCT-FEM MODELS

Cabril dam was used as the case study. Cabril dam was built in the 1950's and is the highest Portuguese arch dam, being one of the largest dams in Portugal. Located in the Zêzere River, Cabril dam is a 132 m high double curvature arch dam. The crest is at an altitude of 297 m and its arch is about 300 m long. The central cantilever width ranges from 19 m at the base to 4.5 m below the crest. The structure's transition to the insertion in the foundation was designed to provide a symmetrical shape. The foundation consists on a granite massif of good quality. As for the reservoir, the water surface level ranges from 240 m (minimum required level of operation) to a maximum storage level of 294 m (the maximum flood level is 296.3 m). During the first filling of the reservoir a horizontal cracking phenomena occurred near the crest, at a height of 280-290 m. A concrete swelling process has also been detected in recent years. Cabril dam geometry is presented in Figure 3.1 by its plan, front and cross section views.

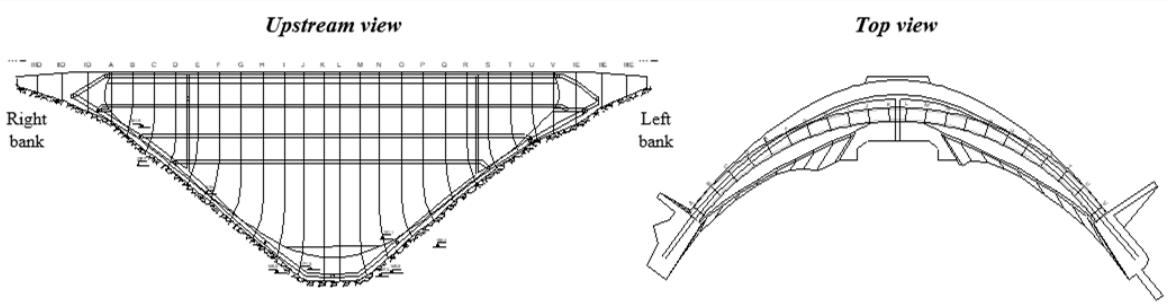


Figure 3.1: Cabril dam. Upstream face and top view

For the use of HSCT-FEM hybrid models, results from a FEM model are necessary, specifically, in what is related to the developed model applied for the Cabril dam case study, it is necessary results from the HP and SW elastic effects, therefore, the phases of construction are not accounted for and the estimation of the creep effect, as mentioned before, is made by applying, to the elastic component, the creep coefficient [4]. The FEM model is also necessary for the results comparison between HSCT-FEM and FEM models. Figure 3.2 presents the adopted model.

The presented FEM model used isoparametric 20 nodes elements with 27 Gauss points for the numerical integration. Since one of the main objectives is to make an accurate effect separation, in order to isolate the swelling effect from the observed results and to verify if this isolated effect resulting from the hybrid HSCT-FEM separation of effects is correct, the results from it must also be coherent with the results from the FEM model. Therefore, to use de FEM to calculate the swelling effect the FEM model has to be verified first. To verify the model, the swelling action has to be calculated for the accumulated period from the construction until the present date and the results compared to those read on the isolated strain gauges. The FEM was used to calculate the swelling reactions action, this program used the thermal and hygrometric fields histories, in the dam body (the program considered the temperatures and humidity observed in both upstream and downstream faces and the equations that govern the heat and humidity fluxes in concrete), and, with the knowledge of the variables that govern the swelling reactions kinetic, the accumulated swelling field was calculated. Figure 3.3 (right) presents the accumulated

swelling field calculated by the FEM, whereas, Figure 3.3 (left) presents the accumulated swelling observed in the isolated strain gauges scattered throughout the dam body.

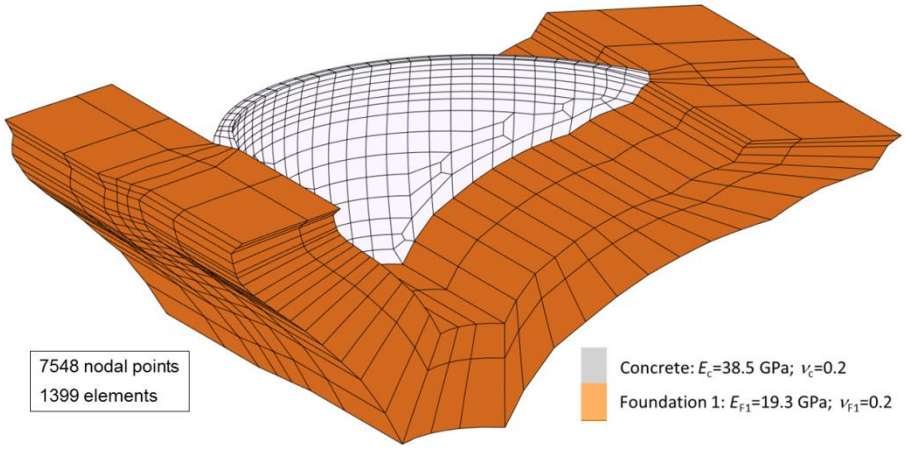


Figure 3.2: Cabril dam FE model.

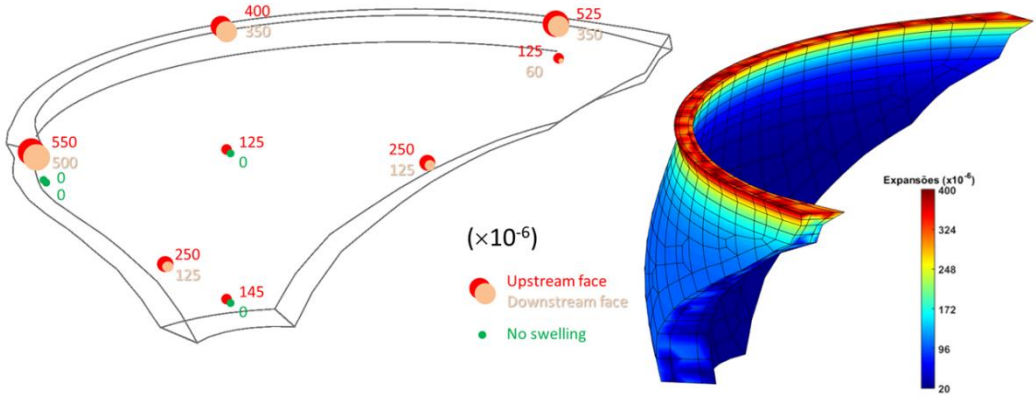


Figure 3.3: Observed values of accumulated swelling from 1952 to the present date. Results from the isolated strain gauges scattered across the dam body

It should be noticed that in the present model is assumed a separation of creep and swelling damage mechanisms, so, as a simplification, it is considered that these phenomena are decoupled. However, it is taken into account that swelling damage (cracking of aggregates) may increase the apparent visco-elastic properties of concrete (creep is assumed to be twice the predicted creep for undamaged concrete) that comes exclusively almost from the cement paste. Both creep and cracking produce relaxation of stresses and change the internal equilibrium and related displacements that cannot be considered with this model.

As is possible to observe, comparing both images from Figure 3.3, there is a coherency between both strain fields. The values obtained from the FEM for the upstream face are mostly higher than those from the downstream face, just like it is observable in the isolated strain gauges, additionally, the highest values calculated by the FEM and observed by the isolated strain gauges are about the within the same scale, around $500\times10^{-6}$. These results validate the adopted FEM model capability to calculate the deformed shape resulting from the swelling reactions load.

The present paper presents the measured displacements histories by the use of the geodetic method and the levelling method. The geodetic method is associated with the horizontal displacements while the levelling method is related to the vertical displacements.

For the observed dam points a HSCT-FEM model was considered with the following characteristics: (i) two exponential functions are used to represent the HP elastic effect with $c_f$ values of 20 and 25 when considering radial displacements and 15 and 20 when considering the vertical displacements (Equation

4), the *a* parameter is previously locked so it can be adjusted to the FEM calculated results; (ii) the temperature effect is represented by observed air temperature at the site considering a 22 days delay to represent the heat flow from the air to the concrete core (Equation 5); (iii) the HP creep effect is simulated by the creep coefficients application to the elastic response, for the monthly water level history discretization in constant intervals, and considering a concrete material with a Bazant and Panula creep law [4] in which: $E_0$ = 38 GPa, $\phi_1$ = 3.0, $\beta$ = 0.05, $m$ = 0.4 and $n$ = 0.25, matching a concrete moderately damaged by swelling (Equation 11 and Figure 2.4a) [5-6]; (iv) the SW creep effect is determined with the creep coefficients application to the elastic displacements estimated by the FEM for the SW action (Equation 14 and Figure 2.4b); (v) time effect related to swelling is given by the sigmoid shaped curve which is characterized by the expression presented by Equation 18 considering an half-swelling time of 15,000 days (approximately 40 years).

Figure 3.4 presents the HSCT-FEM results for the radial displacements at the geodetic mark located at the arch centre, at 295 m of elevation (near the crest). From its analysis is possible to verify the good adjustment HSCT-FEM obtained in the HP elastic effect and temperature effect diagrams (figure's top left and right diagrams, respectively). In the first, as the water level increases, the downstream radial displacement increases, with an approximate maximum value around 40 mm (for the maximum reservoir water level); in the second, the maximum yearly average displacement for the winter cooling is approximately 10 mm towards the downstream direction and is approximately -7.5 mm (upstream direction) for the summer warming. The temperature effect follows a harmonic behaviour.

In the effects separation graph (Figure 3.4 centre graph) is observable, over time, a good adjustment between the LSM displacements and the observed values. The SW creep effect component displays a shape similar to what is presented in Figure 2.4b, although, compared with the other effects, the radial component is negligible. In the time effects graph, over time, the HP elastic effect component follows the water level variation with displacements in the downstream direction.

The temperature effect component over time has a harmonic variation following approximately the annual air temperature variation, although there is a 22 day phase shift between the temperature variation and the structural response in terms of the radial displacements. The winter cooling provokes radial displacements towards downstream while the summer warming provokes displacements towards the upstream direction.

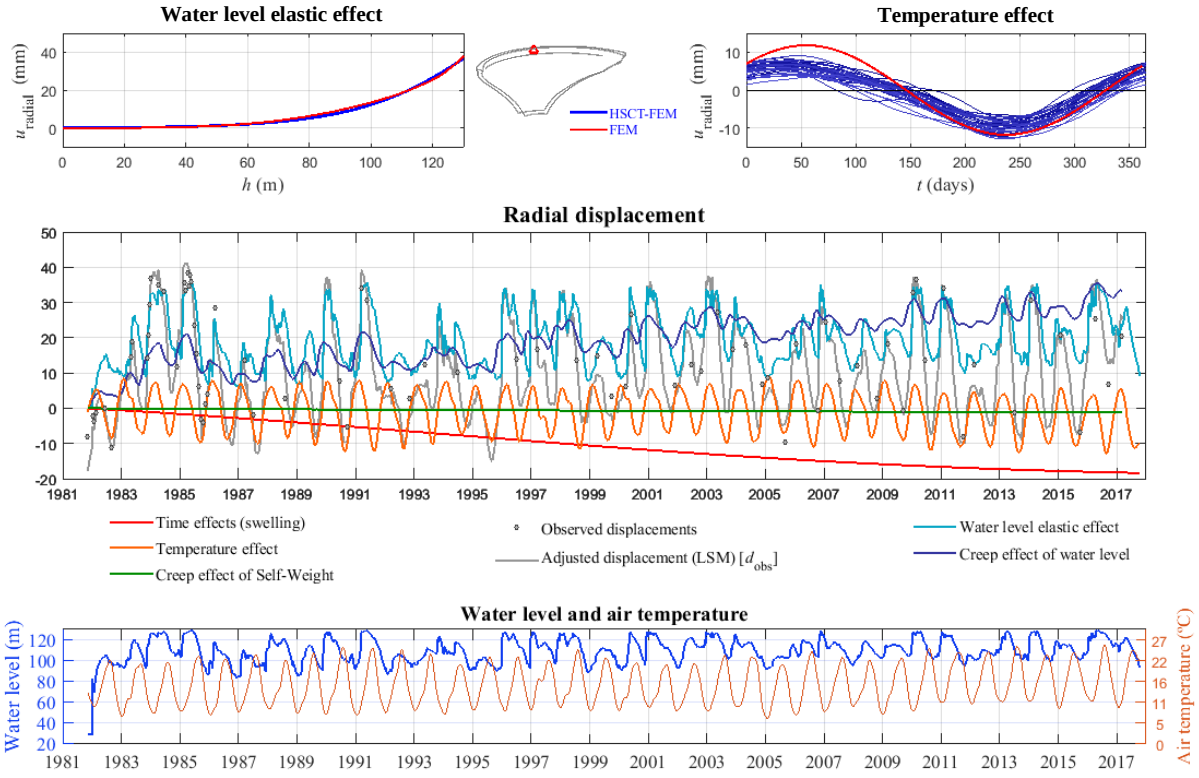


Figure 3.4: Separation of effects and comparison between HSCT/FEM. Radial displacement analysis at the geodetic mark located on block RS, near the crest, at the arch centre, at elevation 295 m. DamSafe3.0 program outputs

The HP creep effect component variation presents, as expected, an increase over time with a 30 mm maximum value towards the downstream direction. The swelling time effect is directed upstream with its accumulated radial displacements in the 20 mm vicinity for the period between 1980 and 2018.

The HSCT-FEM effects separation results are compared with the FEM results in what accounts for the influence lines and the deformed shape. Therefore, Figure 3.5a compares the radial displacements observed by the geodetic method with the FEM results for the radial displacements (displacement fields) and the respective deformed shape for the swelling effect between 1980 and 2018. Figure 3.5b compares the vertical displacements observed by the levelling method with the FEM vertical displacements results. Figure 3.5 presents the swelling fields obtained by the HSCT-FEM statistical model and by the FEM numerical model. In the image it is observable greater radial displacements at the crest in the upstream direction with higher values near the arch's centre and decreasing both towards the embankments and towards the foundation. The vertical displacements display a similar distribution throughout the dam body, with the highest values obtained near the arch's centre at the crest. Through Figure 3.5 results analysis is observable a global agreement between HSCT-FEM and the FEM results. The HP elastic effect displays great similarity between the displacement fields obtained by the HSCT-FEM model and the FEM model. For example, at the arch centre cantilever near the crest, the obtained radial displacement value, resulting from the HSCT model, is around 18 mm, something very similar to what was obtained by the FEM. Similarly, for the vertical displacements, the 11 mm obtained at the centre cantilever near the crest is also within the calculated by FEM for the same location.

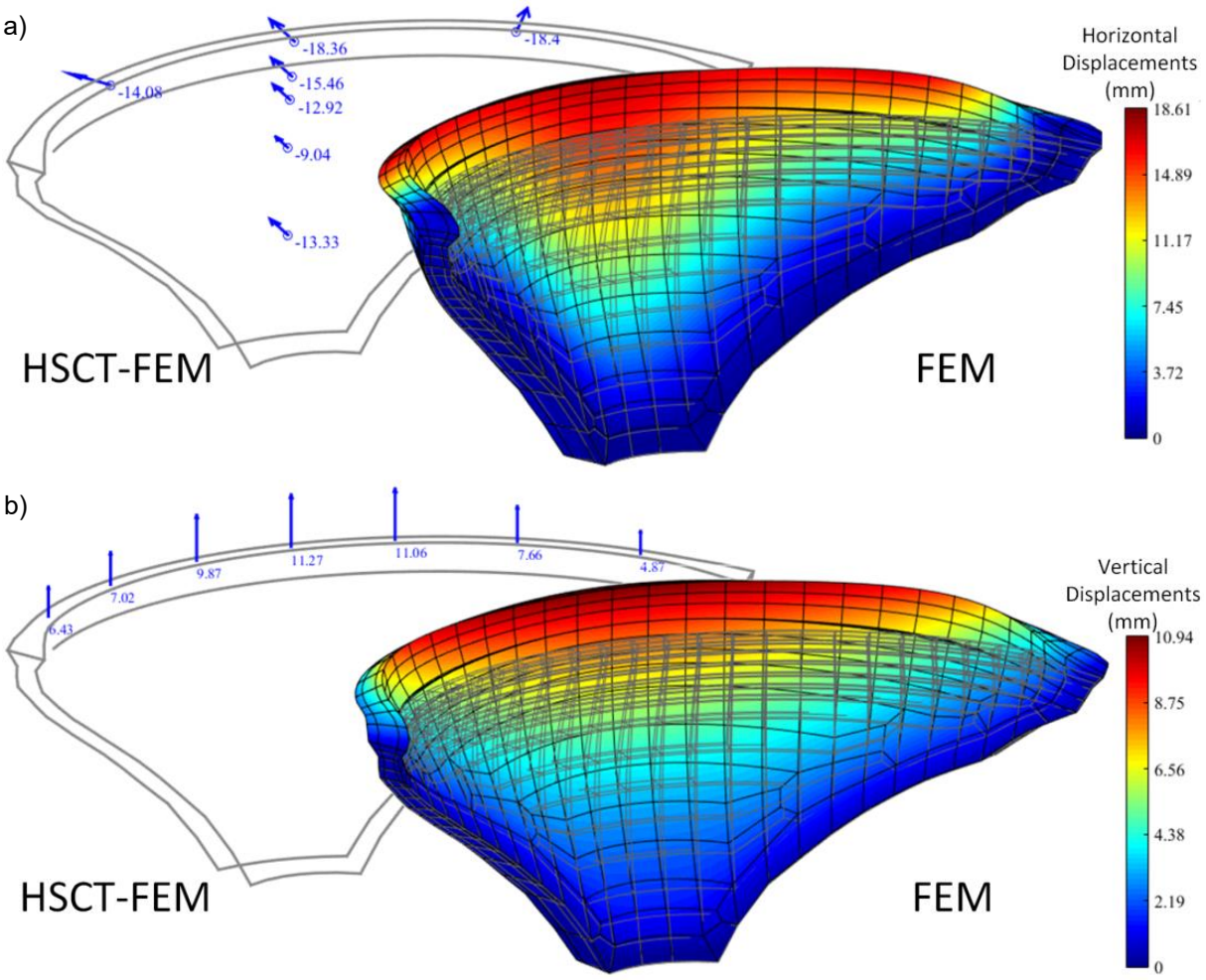


Figure 3.5: Swelling effect. HSCT-FEM and FEM results comparison. a) Radial displacements. b) Vertical displacements. DamSafe3.0 results

## 4. CONCLUSIONS

The methodology presented, using hybrid HSCT-FEM separation of effect models, considering a creep function for a concrete affected by swelling was able to estimate a swelling reactions field based on the observed displacements histories. Additionally, the swelling field obtained is similar to the one produced by the FEM. The mentioned FEM model was verified by the calculation of the swelling action and its comparison with the observed results obtained in the isolated strain gauges scattered throughout the dam body. The results obtained were similar which validated the adopted FEM model.

## 5. REFERENCES

[1] Oliveira S (2000) Modelos para análise do comportamento de barragens de betão considerando a fissuração e os efeitos do tempo. Formulações de dano. PhD thesis, FEUP

[2] Willm G, Beaujoint N (1967) Les méthodes de surveillance des barrages au service de la Production Hidraulique d'Electricité de France; Problèmes anciens e solutions nouvelles. In the Proceedings of the IX ICOLD Congress, Istanbul, R.30, Q.34

[3] Larive G (1997) Apports combinés de l'expérimentation et de la modélisation à la compréhension de l'alcali-réaction et de ses effets mécaniques. PhD thesis, École Nacional de Ponts et Chaussées

[4] Bazant ZP, Panula L (1979) Practical prediction of time dependent deformations of concrete. Materials & Structures

[5] Esposito R, Anaç C, Hendriks M, Çopuroğlu O (2016) Influence of the Alkali-Silica Reaction on Mechanical Degradation of Concrete. Journal of Materials in Civil Engineering 28(6)

[6] Abd-Elssamd A, Ma ZJ, Le Pape Y, Hayes NW, Guimaraes M (2020) Effect of Alkali-Silica Reaction Expansion Rate and Confinement on Concrete Degradation. ACI Mat. J.117(1): pp. 265:278